Anesthesiology 2005; 103:828–36

Short Hairpin RNA–mediated Selective Knockdown of NaV1.8 Tetrodotoxin-resistant Voltage-gated Sodium Channel in Dorsal Root Ganglion Neurons

Maya Mikami, M.D., Jay Yang, M.D., Ph.D.†*

Background: **Voltage-gated sodium channels comprise a family of closely related proteins, each subserving different physiologic and pathologic functions. NaV1.8 is an isoform of voltage-gated sodium channel implicated in the pathogenesis of inflammatory and neuropathic pain, but currently, there is no isoform-specific inhibitor of any voltage-gated sodium channels. The authors explored the possibility of short hairpin RNA–mediated selective knockdown of NaV1.8 expression.**

Methods: **DNA constructs designed to transcribe short hairpin RNA targeting NaV1.8 were created and incorporated into recombinant lentiviruses. The virus-induced selective knockdown of NaV1.8 was examined at the protein, messenger RNA, and functional levels using Western blot, immunohistochemistry, reverse-transcription polymerase chain reaction, and patch clamp electrophysiology.**

Results: **Transduction of HEK293 cells stably expressing NaV1.8 or primary dorsal root ganglion neurons with lentivirus expressing short hairpin RNA resulted in the knockdown of NaV1.8 protein and messenger RNA concentrations. Whole cell patch clamp recordings confirmed decrease in the NaV1.8-mediated current density without changes in other biophysical properties.**

Conclusions: **A selective knockdown of NaV1.8 expression in dorsal root ganglion neurons can be attained by short hairpin RNA delivered with lentivirus. This method may provide a new gene therapy approach to controlling neuronal hyperexcitability and pathologic pain.**

VOLTAGE-GATED sodium channels (VGSCs) play a critical role in determining excitability by supporting the upstroke of the action potential in most excitable tissues. All pore-forming α subunits of the VGSC share a basic protein topology of four repetitive domains (DI–DIV), each containing six transmembrane regions (S1–S6). Thus far, 10 VGSC α subunits, NaV1.1–1.9 and Na_x, have been cloned.[1]

NaV1.8, formerly called the sensory neuron–specific or the peripheral nerve sodium channel type 3 (PN3), is a tetrodotoxin-resistant VGSC α subunit selectively expressed in the dorsal root ganglion (DRG) neurons.[2] A critical role of NaV1.8 in mediating pathologic pain has been suggested by the observation that sensory neuron–specific tetrodotoxin-resistant sodium channel α-subunit knock out mice demonstrated pronounced analgesia to noxious mechanical stimuli and delayed development of inflammatory hyperalgesia while exhibiting generally normal behavior, viability, and fertility.[3] Antisense oligonucleotide–mediated *in vivo* knockdown of NaV1.8 after intrathecal administration inhibited spinal nerve ligation–[4] and intrathecal *N*-methyl-D-aspartate administration–induced[5] neuropathic and inflammatory pain, respectively, which is thought to arise from redistribution of NaV1.8 sensitizing neurons to respond inappropriately to nonnoxious stimuli. NaV1.8 knockout mice also showed deficit in visceral pain and referred hyperalgesia in the intracolonic capsaicin and mustard oil models, suggesting a role of NaV1.8 in mediating spontaneous activity in sensitized nociceptors.[6] Therefore, inhibition of NaV1.8 emerges as an attractive mechanism-based therapy for peripheral and visceral pain of neuropathic and inflammatory origin.

Pharmacologically, VGSCs can be broadly classified into those that are blocked by tetrodotoxin (tetrodotoxin sensitive) and those that relatively insensitive (tetrodotoxin resistant). The PIIIA fraction of μ-conotoxin allows a modest pharmacologic distinction between two members of the tetrodotoxin-sensitive VGSCs as well.[7] However, beyond these limited pharmacologic differences, VGSCs can not be distinguished by any other known drugs. A systematic survey of the effect of drugs commonly used in a clinical setting for treating neuropathic pain on tetrodotoxin-resistant currents flowing through the VGSC in DRG neurons indicated that there are no drugs capable of preferentially blocking these channels over the tetrodotoxin-sensitive channels,[8] although a depolarized membrane potential does increase the sensitivity of the tetrodotoxin-resistant channels to blockade by some drugs. The tetrodotoxin-resistant currents in DRG neurons are mostly carried by the NaV1.8 channels; therefore, a highly selective inhibitor of these channels could be of tremendous clinical importance. In general, a tool for selectively inhibiting the VGSC in an isoform-specific manner will lead to a deeper understanding of the functional role of VGSC isoforms in pain and other critical biologic processes.

RNA interference is a posttranscriptional gene silencing mechanism where a short double-stranded RNA guides the recognition and cleavage of messenger RNA

This article is featured in "This Month in Anesthesiology." Please see this issue of ANESTHESIOLOGY, page 5A.

* Postdoctoral Scientist, † Professor.

Received from the Department of Anesthesiology, Columbia University College of Physicians and Surgeons, New York, New York. Submitted for publication February 4, 2005. Accepted for publication May 27, 2005. Supported by a fellowship from Tohoku University Department of Anesthesiology, Sendai, Miyagi, Japan (to Dr. Mikami), and grant No. RO1 NS045718 from the National Institutes of Health, Bethesda, Maryland (to Dr. Yang).

Address reprint requests to Dr. Yang: Department of Anesthesiology, Columbia University College of Physicians and Surgeons, 630 West 168th Street, New York, New York 10032. Address electronic mail to: jy2029@columbia.edu.

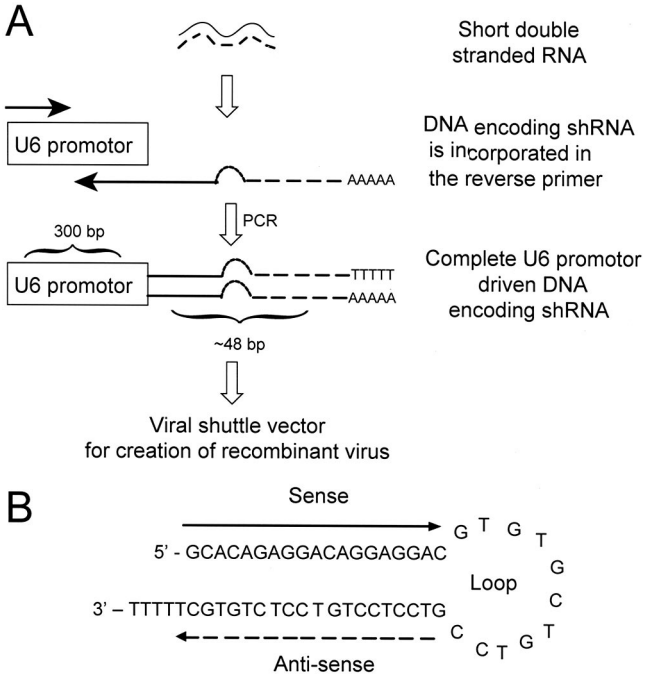

Fig. 1. Creation of a U6 promoter–driven DNA construct designed to express short hairpin RNA (shRNA). (*A*) A double-stranded small interfering RNA (*solid and dashed lines*) designed against a specific sequence of the target protein is joined by a short loop and flanked by the AAAA transcription termination sequence. The nucleotide starts with a *G* immediately after the U6 promoter, thus allowing the Pol III enzyme to precisely initiate transcription at the first base of the sense strand. The entire linear DNA sequence is incorporated into a reverse primer and a complete U6-driven shRNA-expressing construct amplified by polymerase chain reaction (PCR). (*B*) A schematic representation of NaV1.8 (323)-targeting shRNA sequence with the sense sequence concatenated to the antisense sequence by the loop linker. The actual reverse primer will be complimentary to the shown sequence with an addition of 24–base pair (bp) 3′ extension for priming off the 3′ U6 sequence.

(mRNA; reviewed in Meister and Tuschl[9]). Short hairpin RNA (shRNA) is a variant of this approach where a pseudo–double-stranded RNA joined by a short linker results from a hairpin folding of the RNA transcribed from a DNA template.[10] This method of DNA template–based gene silencing is robust and overcomes a fundamental limitation of the transient nature of a true double-stranded RNA–based gene silencing. Despite the flurry of RNA interference work targeting various proteins within the past several years, reports of successful knockdown of ion channels are few.[11–13] We explored the use of this technology to determine whether an isoform-selective knockdown of VGSC can be accomplished. In particular, we investigated whether the NaV1.8 α subunit of the VGSC can be knocked down in the DRG neurons.

Materials and Methods

Creation of shRNA-expressing Lentivirus

Nineteen–base pair (bp) targets for short interfering RNA were identified within the coding sequence for rat NaV1.8 according to the guidelines suggested by Gregory J. Hannon, Ph.D. (Professor, Cold Spring Harbor Laboratory, Cold Spring Harbor, New York), at the Hannon Lab Web site.‡ Five NaV1.8 target sequences were chosen corresponding to nucleotide positions (Accession No. 92184) 323–341, 1103–1121, 1500–1518, 3407–3425, and 6033–6051. In addition, a pan-tetrodotoxin–sensitive target designed against a sequence conserved among NaV1.1, 1.2, 1.3, and 1.7 was provided by Peter Shrager, Ph.D. (Professor, Department of Neurobiology and Anatomy, University of Rochester, Rochester, New York). Each target sequence was screened with nucleotide BLAST to confirm that it were complimentary only to the intended target. The sense and the antisense target sequences linked by an 11-bp loop (a short hairpin construct) were incorporated into an oligonucleotide reverse primer designed to amplify the mouse U6 promoter (fig. 1). This polymerase chain reaction (PCR)–based strategy allowed easy incorporation of the shRNA construct down stream of the U6 promoter compared with the conventional subcloning strategy. The PCR products were subcloned into Topo 2.1 vector (Invitrogen, Carlsbad, CA), sequenced to confirm the fidelity of the product, and then restriction enzyme digested with *Spe*I/*Not*I to put the U6-shRNA expression cassette into the pLL3.7 lentivirus shuttle vector kindly provided by Van Parijs, Ph.D. (Assistant Professor of Biology, Center for Cancer Research, Massachusetts Institute of Technology, Cambridge, Massachusetts).

Lentivirus was produced by a triple transfection of shRNA-pLL3.7, pΔ8.9, and pVSVG as described.[14] In brief, pLL3.7 and packaging vectors were cotransfected into HEK293FT cells using Lipofectamine 2000 (Invitrogen); supernatant was collected after 48 h and passed thorough a 0.45-μm filter to remove debris. The virus titer was increased approximately 20-fold by ultrafiltration (Amicon Ultra 100,000 MW cutoff; Millipore Corporation, Bedford, MA) of the supernatant. An approximate viral titer was determined by infecting HEK293 cells with serial dilutions of the final virus suspension and counting the number of fluorescent cells 48 h after infection. We typically obtained titers of 2–5 $\times$ 10^6 infectious units/ml starting from one 10-cm plate of HEK293FT cells. Further information about the pLL3.7 vector and lentivirus creation can be found at Van Parijs Lab Homepage.§

Rat Neonatal Dorsal Root Ganglia Culture

Dorsal root ganglia cultures were prepared as previously described.[15] Dorsal root ganglia were dissected from postnatal days 1–5 Sprague-Dawley rat pups and

‡ Available at: http://www.cshl.org/public/SCIENCE/hannon.html. Accessed April 15, 2005.

§ Available at: http://csbi.mit.edu/rnai/vector. Accessed April 15, 2005.

digested with 0.25% collagenase and 0.25% trypsin (37°C for 15 min) followed by 0.52 mg/ml soybean trypsin inhibitor and 0.04 mg/ml DNase. After mechanical trituration in Opti-MEM medium (Invitrogen), lentivirus was added to the cell suspension and plated on a polyornithine and laminin–coated 35-mm plastic dish. The medium was changed to Neurobasal (Invitrogen) supplemented with 2% fetal bovine serum and 50 ng/ml 2.5S nerve growth factor 4 h after transduction and maintained at 37°C in a humidified 95% air–5% CO_2 incubator until used for experiments. Electrophysiologic experiments were limited to cells in culture for less than 48 h to limit neurite extension and minimize problems with poor spatial clamp. The animal usage protocol was approved by the Institutional Animal Care and Use Committee of Columbia University (New York, New York).

Immunocytochemistry

Serum from rabbits immunized with N-terminal KLH-conjugated peptide (C)EDEVAAKEGNSPGPQ[16,17] (Genmed Synthesis Inc., San Francisco, CA) was column affinity purified following the manufacturer's recommended protocol (Pierce Biotechnology, Rockford, IL). Cryostat sections (10 μm) of 4% paraformaldehyde fixed, 20% sucrose cryoprotected, and embedding compound (O.C.T.; Sakura Finetek U.S.A. Inc., Torrance, CA)–mounted frozen adult or neonatal DRG neurons were blocked in 10% normal goat serum–phosphate buffered saline with 0.2% Triton X-100, exposed to anti-NaV1.8 affinity purified antibody (1:100) in 2% normal goat serum–phosphate buffered saline with 0.2% Triton X-100 overnight at 4°C, washed, and reacted with Alexa Fluor 528 conjugated goat anti-rabbit secondary antibody (1:500; Molecular Probes, Eugene, OR) for 1 h at room temperature. For cultured DRG, the medium was aspirated, washed with phosphate buffered saline, fixed in 4% paraformaldehyde for 15 min, and processed as described above for DRG sections, except primary antibody exposure was for 2 h at room temperature.

The immunofluorescent images were captured on an Olympus IX50 inverted microscope (Olympus, Melville, NY) using a Cooke SensiCam cooled charge-coupled device camera (Cooke Corporation, Romulus, MI) driven by IP Lab software (Scanalytics Inc., Fairfax, VA). The quantification of the immunoreactive fluorescent signals was achieved through a calibration curve for fluorescence intensity detected by the camera *versus* true fluorescence signal created using 505/515-nm and 580/605-nm fluorescent bead standards (InSpeck; Molecular Probes).[18] Images from the experiments were captured adjusting the shutter duration to assure nonsaturation of the pixels but maximally utilizing the full dynamic range of the digitizer. Finally, the actual fluorescence intensity detected by the camera was corrected by the calibration curve. For clearer presentation, pseudocoloring and contrast enhancement of the images were accomplished in Adobe Photoshop (Adobe Systems Inc., San Jose, CA).

Western Blot

Cells were harvested in ice-cold phosphate-buffered saline, and cell pellets were immediately processed in ice-cold lysis buffer (1% Nonidet P40, 10 mM Tris pH 7.6, 50 mM NaCl, 30 mM NaPPi, 50 mM NaF, 0.5% sodium deoxycholate, and 0.1% sodium dodecyl-sulfate) containing freshly added protease inhibitor (Complete; Roche Applied Science, Indianapolis, IN) for 30 min on ice. Lysed samples were centrifuged at 5,000*g* for 15 min. The supernatant was combined with sodium dodecyl-sulfate sample buffer and incubated at 100°C for 5 min before loading on a 6% or 10% sodium dodecyl-sulfate-polyacrylamide gel. After electrophoresis and transfer to a nitrocellulose membrane (BioRad, Hercules, CA), the membrane was probed with an affinity purified polyclonal anti-NaV1.8 primary antibody, reacted with the horseradish peroxidase–conjugated anti-rabbit secondary antibody, and visualized after reaction with Western Lightning chemiluminescence reagent (NEN Life Science Products, Boston, MA).

Reverse-transcription PCR

Total RNA from cultured DRG neurons 48 h after lentiviral infection or isolated DRG neurons from neonatal rats was extracted using TRIzol Reagent (Invitrogen) and treated with Amplification Grade DNAse I (Invitrogen) to remove genomic DNA contamination. NaV1.8 and NaV1.9 primers used for reverse-transcription PCR (RT-PCR) were described previously.[19,20] Neuron-specific enolase was used as an internal control of input RNA from neurons. Rat neuron-specific enolase forward (5′-TTGGACTCCCGTGGGAATCC-3′) and reverse (5′-ACAGAGAGGCCTGAGCTGATG-3′) primers amplified a 218-bp product that corresponds to nucleotides 167–364 (Accession No. NM139325). Enhanced green fluorescence protein (EGFP) served as a lentiviral expression control. A 400-bp EGFP RT-PCR product corresponding to nucleotides 3820–4200 of the pLL3.7 vector was amplified using forward (5′-ATGCCACCTACGGCAAGCTGA-3′) and reverse (5′-GTGGCGGATCTTGAAGTTCAC-3′) primers.

The SuperScript One-Step RT-PCR (Invitrogen) was used, and PCR conditions for each primer pair were optimized empirically. For example, amplification condition for NaV1.8 using the Stratagene Robocycler thermocycler (Stratagene, La Jolla, CA) was reverse transcription at 55°C for 30 min followed by heat inactivation of the reverse-transcriptase enzyme at 94°C for 5 min, denaturation at 94°C for 30 s, annealing at 59°C for 60 s, and extension at 72°C for 60 s. Amplification was performed for 40 cycles and the final 72°C extension for an additional 10 min. We chose a protocol that allowed robust nonsaturating amplification from 50 ng of starting total RNA because the amount of RNA isolated from DRG

cultures was limited. Amplification products were separated on an agarose gel, and images were digitized and quantified by densitometry using the LabWorks 4.0 software (UVP BioImaging Systems, Upland, CA).

Electrophysiology

Whole cell patch clamp recordings were obtained from cultured DRG (24–48 h after plating) using 1.5-mm (OD) glass patch electrodes filled with 140 mM CsFl, 10 mM NaCl, 1 mM EGTA, 10 mM HEPES, and 2 mM Na_2-adenosine triphosphate, pH 7.3. The extracellular solution consisted of 100 mM choline-Cl, 40 mM NaCl, 2.8 mM KCl, 10 mM tetraethylammonium-Cl, 3 mM $CaCl_2$, 1 mM $MgCl_2$, 0.5 mM $CdCl_2$, 1 mM 4-aminopyridine, and 10 mM glucose, pH 7.4 with 1 μM tetrodotoxin. The theoretical E_{Na} was +23.5 mV (assuming $[Na]_o$ activity coefficient of 0.88),[21] and the decreased Na^+-driving force greatly enhanced our ability to obtain satisfactory spatial clamp. An Axopatch 200B amplifier controlled by the pClamp Version 9.0 software (Axon Instruments Inc., Union City, CA) was used. Cells were held at −120 mV and prepulsed to −50 mV for 500 ms before stepping to the test voltages (−60 to +60 mV). The prepulse protocol taking advantage of the difference in the rate of inactivation largely eliminated the NaV1.9 contribution to the tetrodotoxin-resistant current.[22] The cell capacitance and the series resistance were compensated electronically, and the residual uncompensated transient current was subtracted using the P/4 protocol. Cells were selected based on the completeness of data availability, adequacy of voltage clamp, and access resistance.

The peak current magnitudes were measured from the family of current traces and plotted as the current–voltage curve. The normalized conductance–voltage curve for each cell was constructed from the measured current magnitudes, cell input capacitance, and the experimentally determined reversal potential. The final curve was fit (Origin Version 6.0; Microcal Software Inc., Northampton, MA) with a standard two-state Boltzmann equation:

$$g(V) = g_{max}/(1 + \exp[(V - V_{1/2})/\text{slope}]),$$

where g(V) is the voltage-dependent conductance, g_{max} is maximal conductance, V is membrane voltage, $V_{1/2}$ is half-activation voltage, and slope is a measure of the voltage sensitivity.

Statistical Tests

The two-tailed Mann–Whitney U test was used for comparison of the means (immunocytochemistry fluorescence intensity and electrophysiologic parameters). The tests were considered significant at $P < 0.05$.

Results

ShRNA constructs targeting different VGSC α subunits were created as outlined in figure 1. Two of the constructs targeted tetrodotoxin-sensitive α subunits, whereas the others targeted NaV1.8 differing in the exact nucleotide targeted within the coding sequence for this gene. The nomenclature given to the shRNA constructs created and the respective targeted nucleotides are listed in table 1. All constructs were designed to express the shRNA from the U6 promoter and a coexpression of the EGFP reporter protein from a second cytomegalovirus promoter–driven expression cassette.

Table 1. Short Hairpin RNA Constructs Created and Their Nomenclature

Name	Accession No.	Nucleotides	Targets
Pan-TTXs	X03639	5622	NaV1.1, 1.2, 1.3, 1.7
NaV1.2	X03639	3358	NaV1.2
NaV1.8 (323)	X92184	323	NaV1.8
NaV1.8 (1103)	X92184	1103	NaV1.8
NaV1.8 (1500)	X92184	1500	NaV1.8
NaV1.8 (3425)	X92184	3425	NaV1.8
NaV1.8 (6033)	X92184	6033	NaV1.8

The short hairpin RNA target sequences were chosen corresponding to the nucleotide numbers of the denoted complementary DNA Accession numbers. The individual constructs are denoted by the nomenclature used in the text and figures.

Pan-TTXs = pan-tetrodotoxin sensitive.

First, we sought to demonstrate a selective knockdown of the NaV1.8 protein. To this end, we created a stable cell line expressing the NaV1.8 protein by transfection followed by G418 selection. Figure 2 is an immunocytochemical (A1) and a Western blot (A2) confirmation of the proper expression of NaV1.8 immunoreactive protein of the expected molecular mass (> 260 kd) in the NaV1.8-HEK293 cell line. Infection of this cell line with the shRNA/EGFP-expressing lentivirus resulted in a decrease in the anti-NaV1.8 antibody immunoreactive band detected by a Western blot. As expected, lentivirus only expressing the EGFP reporter or the pan-tetrodotoxin–sensitive shRNA designed to knock down the tetrodotoxin-sensitive α subunits did not inhibit the NaV1.8 protein expression. Of the five shRNA/EGFP constructs targeting the NaV1.8, all demonstrated significant reduction in the immunoreactive protein band except for the NaV1.8 (1103) construct (fig. 2B). The GFP immunoreactivity (fig. 2B, bottom) served as the protein loading control. The protein knockdown was time-dependent, requiring 24 h for a maximal decrease in the anti-NaV1.8 antibody immunoreactive band intensity, although evidence of a target knockdown could be observed as early as 12 h after viral transduction (fig. 2C), even before a significant level of the EGFP reporter expression could be detected. This observation could indicate a different time course of expression of the shRNA from the U6 promoter and the EGFP protein expression from the cytomegalovirus promoter or simply a reflection of the fact that the shRNA transcription product exerts target inhibition before the EGFP trans-

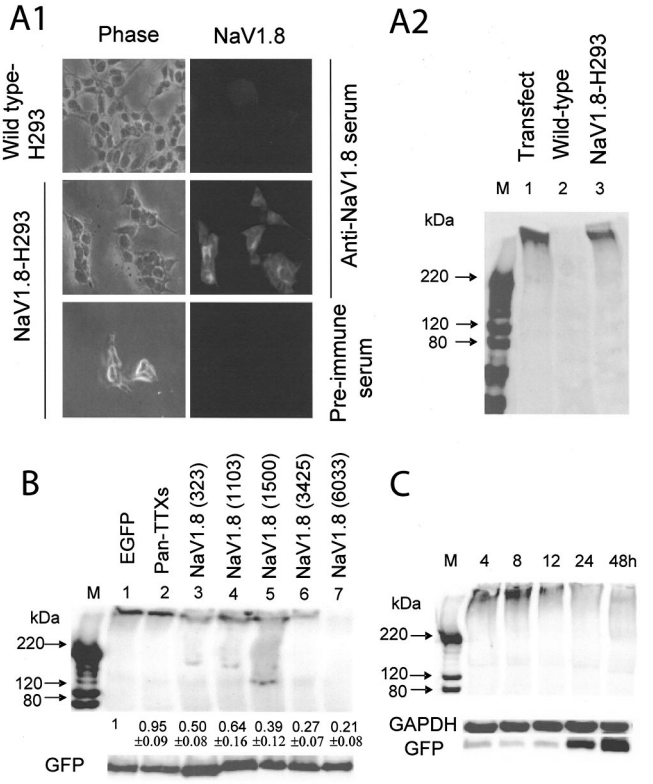

Fig. 2. Time and construct-dependent knockdown of NaV1.8 in an HEK293-NaV1.8 stable cell line. (*A1*) Anti-NaV1.8 immunoreactivity in control wild-type and HEK293 cells stably expressing NaV1.8. (*A2*) Western blot of wild-type HEK293 transiently transfected with NaV1.8-pIRES/neo (*lane 1*), nontransfected wild-type HEK293 (*lane 2*), and HEK293-NaV1.8 stable cell line (*lane 3*). Protein concentrations of the lysates were determined and the lane loading normalized. (*B*) Western blot of cell lysates from HEK293-NaV1.8 cell line 48 h after infection with lentivirus expressing the designated short hairpin RNA/enhanced green fluorescence protein (EGFP) or EGFP alone. The EGFP band serves as a loading and infection efficiency control. Densitometric quantification from six experiments from four separate HEK293-NaV1.8 preparations was performed, and the relative intensities are denoted as numbers (mean ± SEM) below the Western blot. Note the difference in NaV1.8 protein knockdown between different short hairpin RNAs. Pan-TTXs = pan-tetrodotoxin sensitive. (*C*) HEK293-NaV1.8 cell line infected with lentivirus expressing NaV1.8 (6033)-short hairpin RNA/EGFP and harvested at the noted times after infection. Glyceraldehyde-3-phosphate dehydrogenase (GAPDH) serves as a protein loading control. A time-related decrease of NaV1.8 immunoreactivity is concordant with increase of EGFP immunoreactivity that reflects lentiviral expression (however, see Discussion). A significant knockdown was observed 12–24 h after infection.

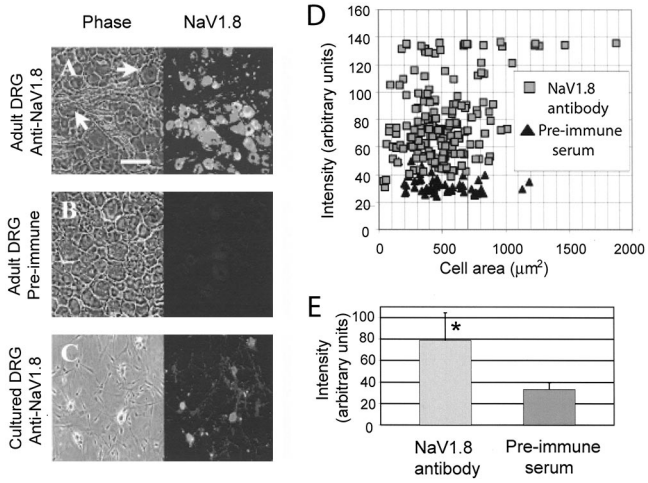

Fig. 3. NaV1.8 immunoreactivity in adult, neonatal and cultured neonatal dorsal root ganglion (DRG) neurons. (*A*) NaV1.8 immunoreactivity in adult DRG section shows preferential distribution in small diameter neurons. *Arrows* indicate the large-diameter DRG neurons. *Scale bar* = 100 μm for all panels. (*B*) Preimmune serum shows no reactivity. (*C*) NaV1.8 immunoreactivity in cultured neonatal DRG is present in all neurons. (*D*) Cell size *versus* immunoreactivity intensity distribution plot confirming no correlation between cell size and immunoreactivity in cultured neonatal DRG. (*E*) Bar plot of immunoreactivity intensity of anti-NaV1.8 antibody-treated (78.7 ± 28.2) and preimmune serum-treated (33.1 ± 6.5) DRG neurons (mean ± SD) (* significant difference). There was no significant difference in immunoreactivity intensity within the anti-NaV antibody treated group when data were separated into cells with areas smaller or larger than 700 μm². Data from eight dishes from two separate cultures.

lation product expression. These results were consistent with the hypothesis that shRNA constructs targeting NaV1.8 inhibited the expression of NaV1.8 protein.

Having confirmed that the shRNA/EGFP constructs knocked down the intended target in a cell line, we investigated NaV1.8 knockdown in DRG neurons. The NaV1.8 protein is preferentially distributed in small-diameter DRG neurons in adult and neonatal rats;[23,24] however, the distribution of the NaV1.8 in cultured neonatal DRG neurons is unknown.[25] Anti-NaV1.8 antibody staining of adult (fig. 3A) and neonatal (data not shown) DRG sections confirmed the expected preferential distribution of the immunoreactivity to small-diameter neurons. Negative-control experiments with the preimmune serum did not show significant immunoreactivity (fig. 3B). In contrast, dissociated neonatal DRG neurons exhibited anti-NaV1.8 immunoreactivity, with no specific neuronal size preference (figs. 3C–E). A potential bias in our analysis of immunoreactivity in cultured neurons could arise if there were a selective loss of large-diameter neurons; however, the observed size distribution of cultured DRG clustering around the smaller cells is consistent with the known predominance of small neurons in adult DRG.[26] More likely is the possibility that NaV1.8 up-regulation in cultured DRG neurons reflects the effect of nerve growth factor in the culture medium because increased concentrations of nerve growth factor are known to increase NaV1.8 expression.[25]

The shRNA/EGFP constructs targeting NaV1.8, NaV1.2, pan-tetrodotoxin–sensitive, or a control construct only expressing the EGFP reporter were expressed in cultured neonatal DRG, and 48 h later, NaV1.8 immunoreactivity was examined by immunocytochemistry (fig. 4A). Neurons expressing the constructs were readily identified by the green fluorescence from the EGFP reporter expression and the relative fluores-

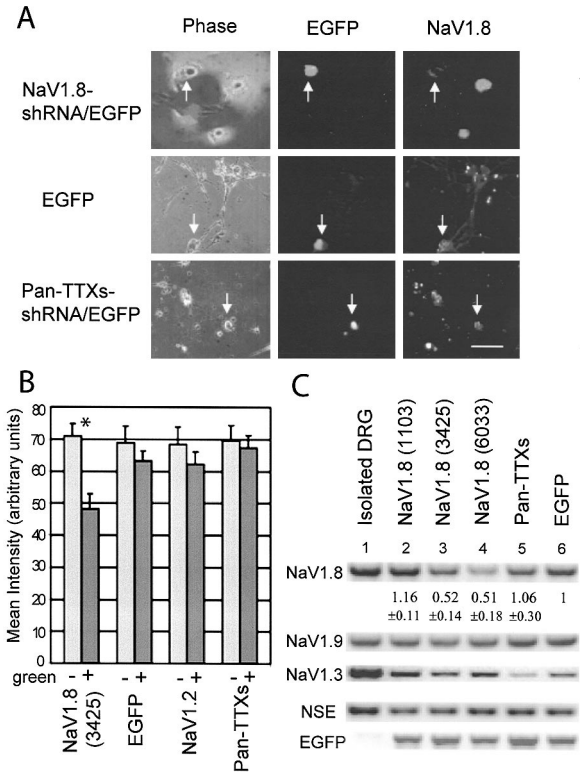

Fig. 4. NaV1.8 immunoreactivity and messenger RNA concentration are decreased only in dorsal root ganglion (DRG) neurons expressing NaV1.8–short hairpin RNA (shRNA)/enhanced green fluorescence protein (EGFP). (*A*) Representative images of DRG cultures expressing the designated constructs. Number of preparations: 18 dishes from 6 separate cultures for EGFP, 6 dishes from 3 cultures for NaV1.8-shRNA/EGFP, and pan-tetrodotoxin–sensitive (Pan-TTXs)–shRNA/EGFP. The images are phase contrast and fluorescent views of EGFP and NaV1.8 immunoreactivity of the same field. The *white arrow* indicates neurons expressing the construct recognized by the green fluorescence (*middle column*). *Scale bar* = 100 μm. (*B*) A bar plot summary (mean ± SEM) of NaV1.8 immunoreactivity intensity of neurons expressing the denoted constructs (green) or control neurons (nongreen). * Significant difference in mean immunoreactivity intensities from n = 50 nongreen and n = 23 green neurons. (*C*) Reverse-transcription polymerase chain reaction (RT-PCR) determination of the denoted messenger RNA abundance in DRG cultures infected by the designated shRNA/EGFP- or only EGFP-expressing lentivirus (*lanes 2–6*). *Lane 1* from acutely isolated neonatal DRG serves as a positive control for the sizes of RT-PCR products. Numbers below the NaV1.8 lane are of relative intensities (mean ± SEM from 7 RT-PCR amplifications from 3 separate DRG preparations) of the RT-PCR products after normalization with respective neuron-specific enolase (NSE) bands. The signal intensity of the EGFP-transduced dish was taken as 1.00.

cence intensity of anti-NaV1.8 antibody immunoreactivity quantified (fig. 4B). Neurons expressing the EGFP reporter alone, pan-tetrodotoxin–sensitive-shRNA/EGFP, or NaV1.2-shRNA/EGFP exhibited the same intensity of anti-NaV1.8 immunoreactivity compared with the nongreen (*i.e.*, nontransduced) cells in the same dish. In contrast, there was a significant reduction in the fluorescence intensity in neurons expressing NaV1.8-shRNA/EGFP. We were unable to perform the reciprocal experiment examining for the level of NaV1.2 protein expression in DRG neurons because we were unable to obtain a selective antibody against NaV1.2 that worked.

We next sought reciprocal evidence for a selective target knockdown by examining whether the NaV1.8-shRNA/EGFP constructs nonspecifically inhibited expression of other VGSC α subunits. Because VGSC subtype-specific antibodies were not available commercially at this time, it was not possible to do the study at the protein level. However, study of the mRNAs encoding sodium channels by RT-PCR provided information on whether the corresponding mRNAs were effectively decreased by shRNA. We tested mRNA concentrations for NaV1.3, NaV1.8, and NaV1.9 after shRNA/EGFP lentivirus transduction of DRG cultures. For this experiment, three NaV1.8 shRNA constructs were used, shNaV1.8 (1103), which demonstrated poor protein down-regulation, and shNaV1.8 (3425) and shNaV1.8 (6033), with effective protein knockdown. Figure 4C demonstrates that two NaV1.8-shRNA/EGFPs selectively diminished the NaV1.8 mRNA concentration in accord with the protein concentration study while leaving the mRNA for nontargeted NaVs intact. In contrast, the pan-tetrodotoxin–sensitive-shRNA/EGFP expression decreased NaV1.3 mRNA. The RT-PCR product for neuron-specific enolase served as a control for the relative amount of nerve cells present in the particular culture dish and the EGFP control for the relative efficiency of lentivirus transduction.

Last, we examined for evidence of knockdown of functional NaV1.8 α subunit by recording sodium currents in cultured DRG neurons. Whole cell patch clamp recordings were obtained from DRG neurons expressing the control EGFP or NaV1.8-shRNA/EGFP constructs with the presence of the green fluorescence again used as evidence for successful transduction. The NaV1.8 (6033) was used for these experiments because this target best reduced NaV1.8 protein and mRNA concentrations among the five constructs tested. The electrophysiologic assay was limited to 48 h after plating the DRG culture to assure adequate spatial clamp because longer time in culture resulted in long neurite extension and poor voltage clamp despite reduction in the Na^+ driving force. Figure 5A shows representative current traces from EGFP– (left) and NaV1.8-shRNA/EGFP–expressing (right) neurons elicited by voltage steps to −60 to +60 mV from a holding potential of −120 mV. In the presence of tetrodotoxin, the resulting family of currents represents tetrodotoxin-resistant current flowing mostly through the NaV1.8 channels. The current–voltage plot (fig. 5B) demonstrated no difference in the voltage dependence of current activation between the large currents from the control neuron and the small residual currents in NaV1.8-shRNA/EGFP–expressing neuron. Further analysis of the currents by quantification of the conductance–voltage plot confirmed this impression (fig. 5C and table 2). The distribution of tetrodotoxin-

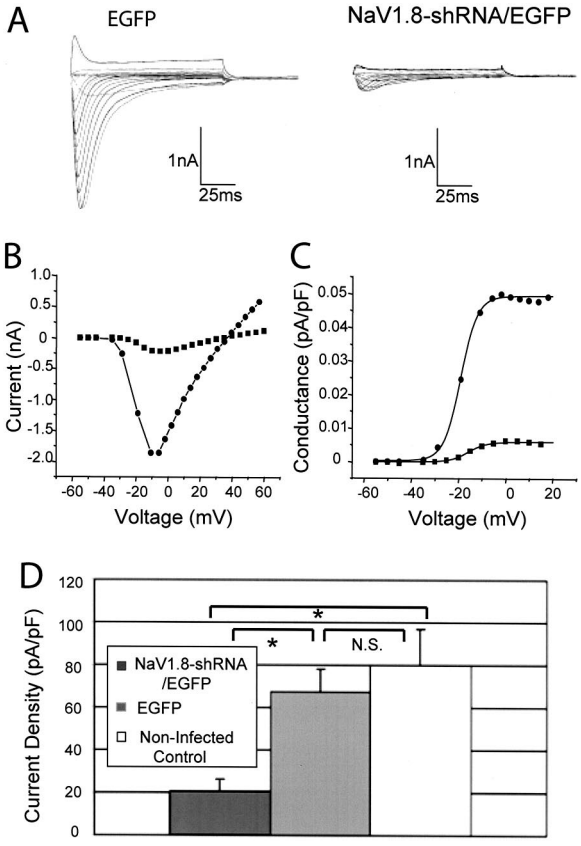

Fig. 5. Electrophysiologic evidence for a knockdown of functional NaV1.8 channels. (*A*) Representative currents activated by a family of depolarizing steps (−60 to +60 mV) in enhanced green fluorescence protein (EGFP; *left*)– and NaV1.8 (3425)-short hairpin RNA (shRNA)/EGFP (*right*)–expressing dorsal root ganglion neurons. (*B*) Current–voltage and (*C*) conductance–voltage plots of the same cells. The fitted parameters were as follows: EGFP (*gray circles*): g_{max} = 5.9 nS, $V_{1/2}$ = −16.7 mV, slope = 3.7; NaV1.8-shRNA/EGFP (*black squares*): g_{max} = 49 nS, $V_{1/2}$ = −19.0 mV, slope = 3.5. (*D*) A bar plot of the mean normalized peak tetrodotoxin-resistant current density for NaV1.8-shRNA/EGFP–expressing (n = 5), EGFP-expressing (n = 13), and noninfected control (n = 7) dorsal root ganglion neurons. *Error bar* represents SE. * Statistical significance at $P < 0.05$ (Mann–Whitney U test). NS = not significant.

resistant current density was significantly decreased in NaV1.8-shRNA/EGFP–expressing neurons (fig. 5D). Thus, we demonstrated a successful shRNA-mediated knockdown of the NaV1.8 α subunit in primary DRG neurons by immunohistochemical, RT-PCR, and patch clamp techniques.

Discussion

Our results demonstrated a successful shRNA-mediated selective knockdown of NaV1.8 protein in a cell line expressing the NaV1.8 protein and also in cultured primary neonatal DRG neurons. To our knowledge, this is the first report of shRNA-mediated knockdown of a VGSC and confirms that this technology enables a highly selective knockdown of a given member of this protein family with high homology not distinguishable by available toxins and pharmacologic agents. Four of the five NaV1.8-shRNAs demonstrated adequate knockdown, whereas one construct did not do so. All five constructs were created following the general guidelines, and it is not clear why one of the five constructs did not exhibit target knockdown. Several factors that may influence the efficiency of RNA interference have been reported,[27,28] *e.g.*, the choice of target site and secondary structure. However, a reliable guideline for constructing the best shRNA has not been established yet. Our limited experience supports the general notion that the RNA interference approach to a target knockdown is more robust and easily attainable with little trial and error compared with the antisense oligonucleotide method.[29] Further experiments with base-mismatched shRNAs are necessary to precisely define the tolerance and fidelity of RNA interference–mediated VGSC knockdown.

Our whole cell patch clamp data from DRG neurons confirmed the reduction in tetrodotoxin-resistant current density in NaV1.8-shRNA/EGFP–expressing neurons. Two methodologic points merit discussion: first, whether the residual current remaining in theNaV1.8-shRNA transduced cells was mediated by the remaining NaV1.8 channels or whether the current could be a contaminating current mediated by the NaV1.9 channels, and second, whether a complete elimination of the functional NaV1.8 protein can be attained.

It is now well recognized that NaV1.9 mediates tetrodotoxin-resistant current in mouse DRG neurons,[30,31] in addition to the NaV1.8. These two channels are encoded by different VGSC genes, but tetrodotoxin alone can not distinguish currents flowing through these distinct channels. However, the two channels exhibit a marked difference in their biophysical properties such as the activation voltage (more depolarized for NaV1.8), inactivation (more positive for NaV1.8), and the recov-

Table 2. Electrophysiologic Parameters Describing the Tetrodotoxin-resistant Sodium Current in Dorsal Root Ganglion Neurons

DRG Neurons	n	Vm at Peak Na Current, mV	$V_{1/2}$ Potential, mV	Reversal Density Factor, mV	Current, pA/pF	Slope, mV
NaV1.8 shRNA/EGFP	5	−23.0 ± 6.4	−20.4 ± 8.3	6.7 ± 7.0	20.4 ± 5.9*	6.4 ± 1.9
EGFP	13	−30.0 ± 2.9	−23.2 ± 2.6	17.3 ± 3.6	67.6 ± 10.4	5.3 ± 0.6
No infection control	7	−27.9 ± 3.3	−24.1 ± 2.5	19.8 ± 2.4	79.9 ± 17.2	4.9 ± 1.1

Data are expressed as mean ± SEM.

* Statistically significant difference between the groups ($P < 0.05$).

DRG = dorsal root ganglion; EGFP = enhanced green fluorescence protein; shRNA = short hairpin RNA; $V_{1/2}$ = half-activation voltage; Vm = membrane voltage.

ery from inactivation (slower for NaV1.8).[31] We used a prepulse to −50 mV for 500 ms before stepping to the respective activation voltages, as described by Tyrrell *et al.*,[22] in an effort to minimize the contamination of the elicited tetrodotoxin-resistant current by NaV1.9. Given the documented current activation in the range of −20 to −10 mV in our cells, we believe the observed current was largely due to NaV1.8. Likewise, the residual tetrodotoxin-resistant current seen in NaV1.8-shRNA–expressing cells was not due to contaminating NaV1.9 but rather reflects current flowing through the remaining NaV1.8 because activation voltage remained very positive, with a $V_{1/2}$ of −20 to −10 mV range, whereas this parameter for NaV1.9 $V_{1/2}$ should have been closer to −60 mV.

Can total inhibition of NaV1.8 be attained? Our electrophysiologic assay was limited to 48 h after plating the DRG neurons because of the technical difficulty of obtaining a satisfactory voltage clamp. However, our Western blot data on NaV1.8-HEK293 cell line demonstrated a complete elimination of the NaV1.8 protein by 24 h after infection with lentivirus expressing the NaV1.8-shRNA constructs. Therefore, at 48 h, the shRNA should have exerted its maximal knockdown, and our inability to electrophysiologically study the neurons at a later time point should not have been a limitation, assuming that the NaV1.8 protein half-life was comparable in the two systems. NaV1.2 expressed in the brain is known to associate with accessory proteins such as contactin,[32] and this association prolongs the protein half-life. NaV1.8 has been demonstrated to interact with the annexin accessory protein, which also prolongs the protein half-life, and increase the channel expression.[33] Although simply waiting longer for the NaV1.8-shRNA to exert its full knockdown may be sufficient to totally inhibit the tetrodotoxin-resistant current in DRG neurons, an alternative strategy to enhance the target knockdown is to simultaneously target the accessory protein.

Although this work focused on NaV1.8 as the target for knockdown based on its likely role in inflammatory and neuropathic pain, it is unlikely that this α subunit is the only VGSC involved in the generation of pathologic pain. A recent study indicates that a peripheral nerve injury resulted in the increased expression of NaV1.3 in DRG and second-order spinal neurons.[34] Isoform selective knockdown of NaV1.3 by shRNA may be a viable approach to preventing central sensitization and neuropathic pain. In fact, a systematic use of the shRNA-based technology that allows a selective knockdown of the homologous α subunits of VGSC, one at a time or in combination, may allow us to decipher the complex interaction between different VGSCs in mediating pathologic pain.

The major advantage of shRNA-mediated knockdown is the fact that the pseudo–double-stranded hairpin RNA is transcribed from a DNA construct allowing for the potential for a prolonged RNA inhibition and knockdown of the target protein. However, plasmid-based shRNA expression has limitations in cases where transfection efficiency is low, especially in mitotically arrested neurons. To solve this problem, we used recombinant lentivirus because they effectively transduce nondividing cells. *In vivo* injection of the shRNA-expressing lentivirus should allow a selective knockdown of the pathogenic target protein, restoring normal excitability in sensitized neurons. Furthermore, lentivirus integration into the host genome should result in a localized perpetual knockdown of the target protein in the infected cells, opening up the exciting possibility of a shRNA-mediated viral vector-based *in vivo* gene therapy for the currently difficult to treat chronic pain of neuropathic and inflammatory origin.

The authors thank Sarah Giardina, Ph.D. (Postdoctoral Research Scientist, Columbia University Department of Anesthesiology, New York, New York), for her comments on the manuscript.

References

1. Goldin AL, Barchi RL, Caldwell JH, Hofmann F, Howe JR, Hunter JC, Kallen RG, Mandel G, Meisler MH, Netter YB, Noda M, Tamkun MM, Waxman SG, Wood JN, Catterall WA: Nomenclature of voltage-gated sodium channels. Neuron 2000; 28:365–8

2. Novakovic SD, Eglen RM, Hunter JC: Regulation of Na channel distribution in the nervous system. Trends Neurosci 2001; 24:473–8

3. Akopian AN, Souslova V, England S, Okuse K, Ogata N, Ure J, Smith A, Kerr BJ, McMahon SB, Boyce S, Hill R, Stanfa LC, Dickenson AH, Wood JN: The tetrodotoxin-resistant sodium channel SNS has a specialized function in pain pathways. Nature Neurosci 1999; 2:541–8

4. Lai J, Gold MS, Kim C, Bian D, Ossipov MH, Hunter JC, Porreca F: Inhibition of neuropathic pain by decreased expression of the tetrodotoxin-resistant sodium channel, NaV1.8. Pain 2002; 95:143–52

5. Parada CA, Vivancos GG, Tambeli CH, deq Ueiroz Cunha F, Ferreira SH: Activation of presynaptic NMDA receptors coupled to NaV1.8-resistant sodium channel C-fibers causes retrograde mechanical nociceptor sensitization. Proc Natl Acad Sci U S A 2003; 100:2923–8

6. Laird JMA, Souslova V, Wood JN, Cervero F: Deficits in visceral pain and referred hyperalgesia in NaV1.8 (SNS/ PN3)-null mice. J Neurosci 2002; 22: 8352–6

7. Safo P, Rosenbaum T, Shcherbatko A, Choi DY, Han E, Toledo-Aral JJ, Olivera BM, Brehm P, Mandel G: Distinction among neuronal subtypes of voltage-activated sodium channels by μ-conotoxin PIIIA. J Neurosci 2000; 20:76–80

8. Brau ME, Dreimann M, Olschewski A, Vogel W, Hempelmann G: Effect of drugs used for neuropathic pain management on tetrodotoxin-resistant Na^+ currents in rat sensory neurons. ANESTHESIOLOGY 2001; 94:137–44

9. Meister G, Tuschl T: Mechanisms of gene silencing by double-stranded RNA. Nature 2004; 431:343–9

10. Hannon GJ, Rossi JJ: Unlocking the potential of the human genome with RNA interference. Nature 2004; 431:371–8

11. Aarts M, Iihara K, Wei W, Xiong Z, Arundine M, Cerwinski W, MacDonald JF, Tymianski M: A key role for TRPM7 channels in anoxic neuronal death. Cell 2003; 115:863–77

12. Splinter PL, Masyuk AI, LaRusso NF: Specific inhibition of AQP1 water channels in isolated rat intrahepatic bile duct units by small interfering RNAs. J Biol Chem 2003; 278:6268–74

13. Dorn G, Patel S, Wotherspoon G, Hemmings-Mieszczak M, Barclay J, Natt FJC, Martin P, Bevan S, Fox A, Ganju P, Wishart W, Hall J: siRNA relieves chronic neuropathic pain. Nucleic Acids Res 2004; 32:e49

14. Zufferey R, Nagy D, Mandel RJ, Naldini L, Trono D: Multiply attenuated lentiviral vector achieves efficient gene delivery in vivo. Nature Biotechnol 1997; 15:871–5

15. Kimpinski K, Campenot RB, Mearow K: Effects of the neurotrophins nerve growth factor, neurotrophin-3, and brain-derived neurotrophic factor (BDNF) on neurite growth from adult sensory neurons in compartmented cultures. J Neurobiol 1997; 33:395–410

16. Amaya F, Decosterd I, Samad TA, Plumpton C, Tate S, Mannion RJ, Costigan M, Woolf CJ: Diversity of expression of the sensory neuron-specific TTX-resistant voltage-gated sodium ion channels SNS and SNS2. Mol Cell Neurosci 2000; 15:331–42

17. Coward K, Plumpton C, Facer P, Birch R, Carlstedt T, Tate S, Bountra C, Anand P: Immunolocalization of SNA/PN3 and NaN/SNS2 sodium channels in human pain states. Pain 2000; 85:41–50

18. Honore P, Rogers SD, Schwei MJ, Salak-Johnson JL, Luger NM, Sabino MC, Clohisy DR, Mantyh PW: Murine models of inflammatory, neuropathic and cancer pain each generates a unique set of neurochemical changes in the spinal cord and sensory neurons. Neuroscience 2000; 98:585–98

19. Dib-Hajj SD, Tyrrell L, Black JA, Waxman SG: NaN, a novel voltage-gated Na channel, is expressed preferentially in peripheral sensory neurons and down-regulated after axotomy. Proc Natl Acad Sci U S A 1998; 95:8963–8

20. Dib-Hajj SD, Fjell J, Cummins TR, Zheng Z, Fried K, LaMotte R, Black JA, Waxman SG: Plasticity of sodium channel expression in DRG neurons in the chronic constriction injury model of neuropathic pain. Pain 1999; 83:591–600

21. Gu XQ, Dib-Hajj S, Rizzo MA, Waxman SG: TTX-sensitive and -resistant Na+ currents, and mRNA for the TTX-resistant rH1 channel, are expressed in B104 neuroblastoma cells. J Neurophysiol 1997; 77:236–46

22. Tyrrell L, Renganathan M, Dib-Hajj SD, Waxman SG: Glycosylation alters steady-state inactivation of sodium channel Nav1.9/NaN in dorsal root ganglion neurons and is developmentally regulated. J Neurosci 2001; 21:9629–37

23. Akopian AN, Sivilotti L, Wood JN: A tetrodotoxin-resistant voltage-gated sodium channel expressed by sensory neurons. Nature 1996; 379:257–62

24. Sangameswaran L, Delgado SG, Fish LM, Koch BD, Jakeman LB, Stewart GR, Sze P, Hunter JC, Eglen RM, Herman RC: Structure and function of a novel voltage-gated, tetrodotoxin-resistant sodium channel specific to sensory neurons. J Biol Chem 1996; 271:5953–6

25. Fjell J, Cummins TR, Dib-Hajj SD, Fried K, Black JA, Waxman SG: Differential role of GDNF and NGF in the maintenance of two TTX-resistant sodium channels in adult DRG neurons. Mol Brain Res 1999; 67:267–82

26. Bennett DLH, Michael GJ, Ramachandran N, Munson JB, Averill S, Yan Q, McMahon SB, Priestley JV: A distinct subgroup of small DRG cells express GDNF receptor components and GDNF is protective for these neurons after nerve injury. J Neurosci 1998; 18:3059–72

27. Van der Krol AR, Mur LA, Beld M, Mol JN, Stuitje AR: Flavonoid genes in petunia: Addition of a limited number of gene copies may lead to a suppression of gene expression. Plant Cell 1990; 2:291–9

28. Aoki Y, Cioca DP, Oidaira H, Kamiya J, Kiyosawa K: RNA interference may be more potent than antisense RNA in human cancer cell line. Clin Exp Pharmacol Physiol 2003; 30:96–102

29. Fire A, Xu S, Montgomery MK, Kostas SA, Driver SE, Mello CC: Potent and specific genetic interference by double-stranded RNA in *Caenorhabditis elegans.* Nature 1998; 391:806–11

30. Tate S, Benn S, Hick C, Trezise D, John V, Mannion RJ, Costigan M, Plumpton C, Grose D, Gladwell Z, Kendall G, Dale K, Bountra C, Woolf CJ: Two sodium channels contribute to the TTX-R sodium current in primary sensory neurons. Nature Neurosci 1998; 1:653–5

31. Cummins TR, Dib-Hajj SD, Black JA, Akopian AN, Wood JN, Waxman SG: A novel persistent tetrodotoxin-resistant sodium current in SNS-null and wild-type small primary sensory neurons. J Neurosci 1999; 19:RC43

32. Kazarinova-Noyes K, Malhotra JD, McEwen DP, Mattei LN, Berglund EO, Ranscht B, Levinson SR, Schachner M, Shrager P, Isom LL, Xiao ZC: Contactin associates with Na+ channels and increases their functional expression. J Neurosci 2001; 21:7517–25

33. Okuse K, Malik-Hall M, Baker MD, Poon W-Y L, Kong H, Chao MV, Wood JN: Annexin II light chain regulates sensory neuron-specific sodium channel expression. Nature 2002; 417:653–6

34. Hains BC, Saab CY, Klein JP, Craner MJ, Waxman SG: Altered sodium channel expression in second-order spinal sensory neurons contributes to pain after peripheral nerve injury. J Neurosci 2004; 24:4832–9